



**1999 AGU Fall Meeting
San Francisco, CA, USA
13–17 December 1998**

Plasma Sheet Access to the Inner Magnetosphere

R. H. W. Friedel

M. D. Henderson

H. Korth

M. F. Thomsen

LOS ALAMOS NATIONAL LABORATORY,

LOS ALAMOS, NEW MEXICO, USA



J. D. Scudder

UNIVERSITY OF IOWA, IOWA CITY, IOWA, USA



The HYDRA results of this paper are the results of NASA funding under grant number NAG 5 2231 and DARA under grant 50 OC 8911 0.

Contents



- A. Overview
- B. POLAR orbit
- C. Instrumentation - Data
- D. Electron Drift Trajectories
- E. The (U,B,K) Theory
- F. Description of plots - plots
- G. Geosynchronous comparison
- H. Summary
- I. References



A. Overview

We present here plasma data from the POLAR HYDRA instrument from three years of data, giving global coverage of the inner magnetospheric region from $L \sim 2$ outward.

Data are mapped along field lines to an equatorial reference plane at constant μ .

This maps out the inner boundary for plasma electrons and ions, and highlights the origin of particles observed by POLAR.

We compare the boundaries to the predicted Alfvén boundaries as a function of the geomagnetic activity index KP.

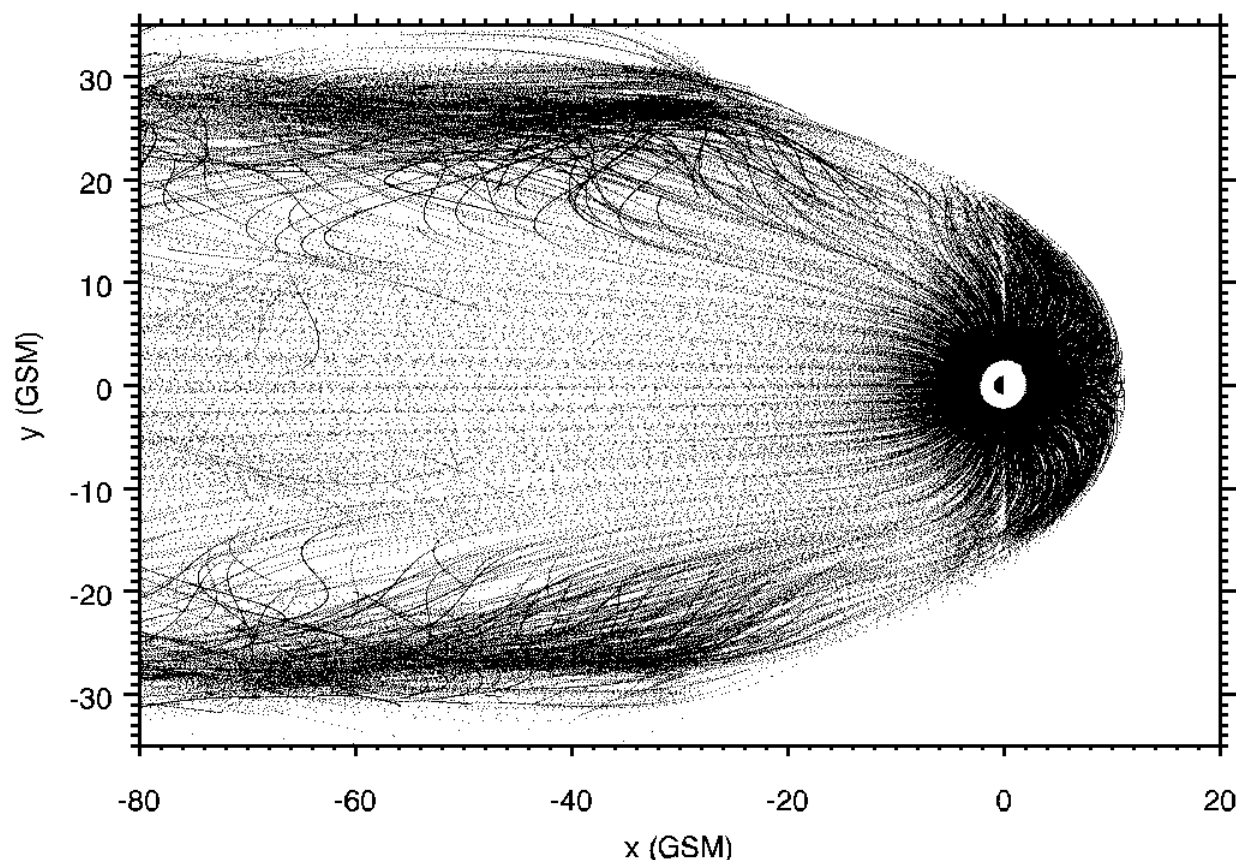
The data are further compared to the geosynchronous “slice” as measured by the Los Alamos Geosynchronous plasma instrument (MPA) which measures the crossing point of the Alfvén boundaries at geosynchronous altitudes.



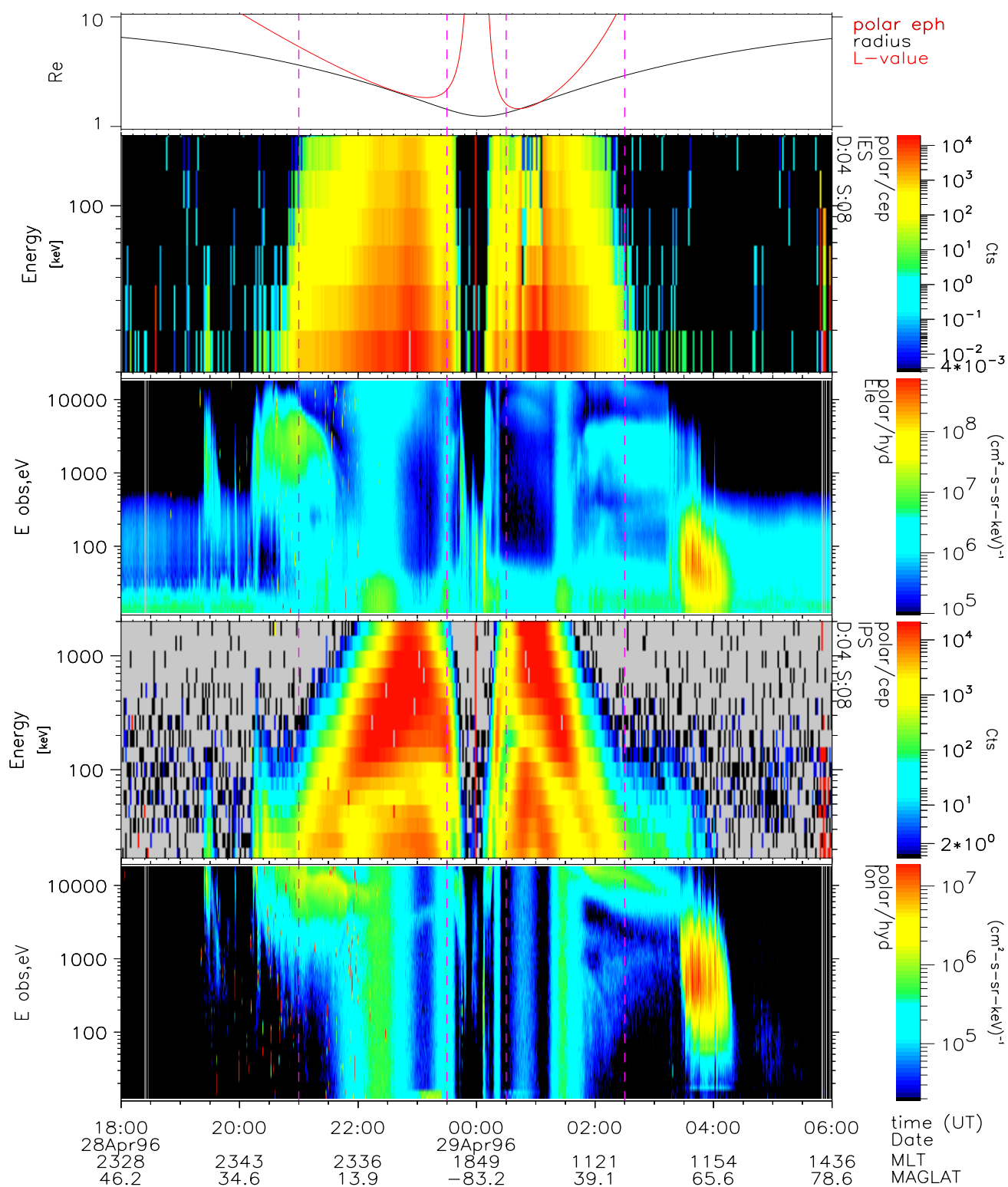
B1. POLAR orbit

POLAR has been operating for 45 months. While most attention has been on boundary crossings and examinations of the cusp, POLAR also offers a continuing coverage of the inner magnetosphere.

POLAR has an elliptical orbit ~ 1.8 to $9 R_E$ at 86° inclination. The spacecraft traverses the inner region field lines four times each orbit, at different MLT and at different magnetic latitudes. All MLT are covered within half a year, and the field lines threading POLAR's orbit cover virtually the whole of the magnetosphere:



B2. Example of POLAR inner magnetosphere pass





C1. Instrumentation - Data

HYDRA for electrons and ions from 20-20000 eV (no composition) [*Scudder et al.*, 1995] for the period March 1996 - December 1998.

The data used are perpendicular electron and ion fluxes that have been corrected for spacecraft charging.

Using the perpendicular local fluxes together with the local magnetic field allows the calculation of the particle's first adiabatic invariant:

$$\mu = \frac{mv_{\perp}^2}{2B} = \frac{E_k}{B} \quad (1)$$

in units of $\frac{eV}{nT}$.

Each spectrum is converted to μ from which a set of 10 fixed interpolated μ are extracted:

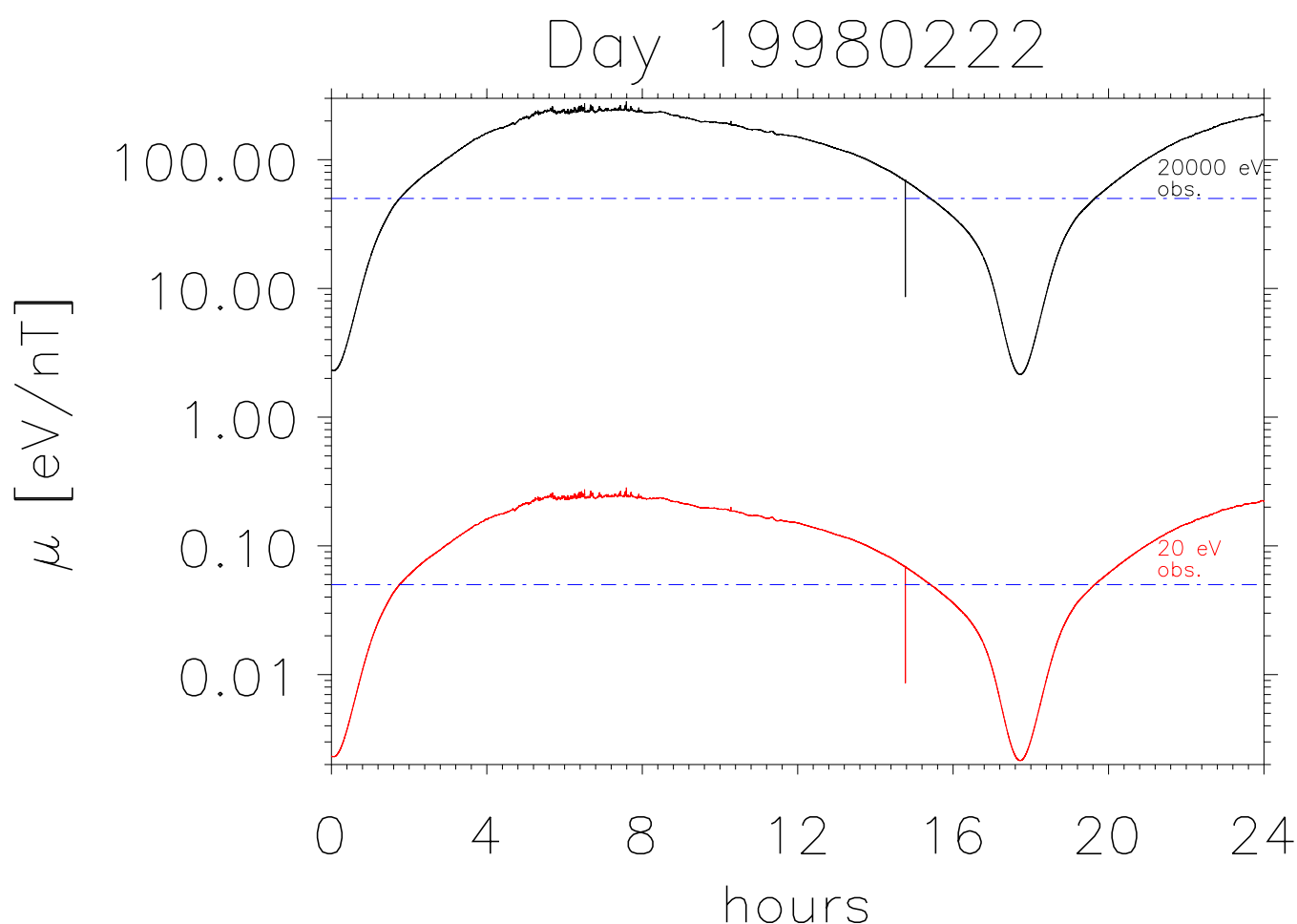
$$[0.05, 0.1, 0.2, 0.5, 1.0, 2.0, 5.0, 10.0, 20.0, 50.0] \frac{eV}{nT}$$

This corresponds to an observed energy range of roughly 7.5 eV to 7.5 keV at geosynchronous orbit.



C2. Data Coverage in μ

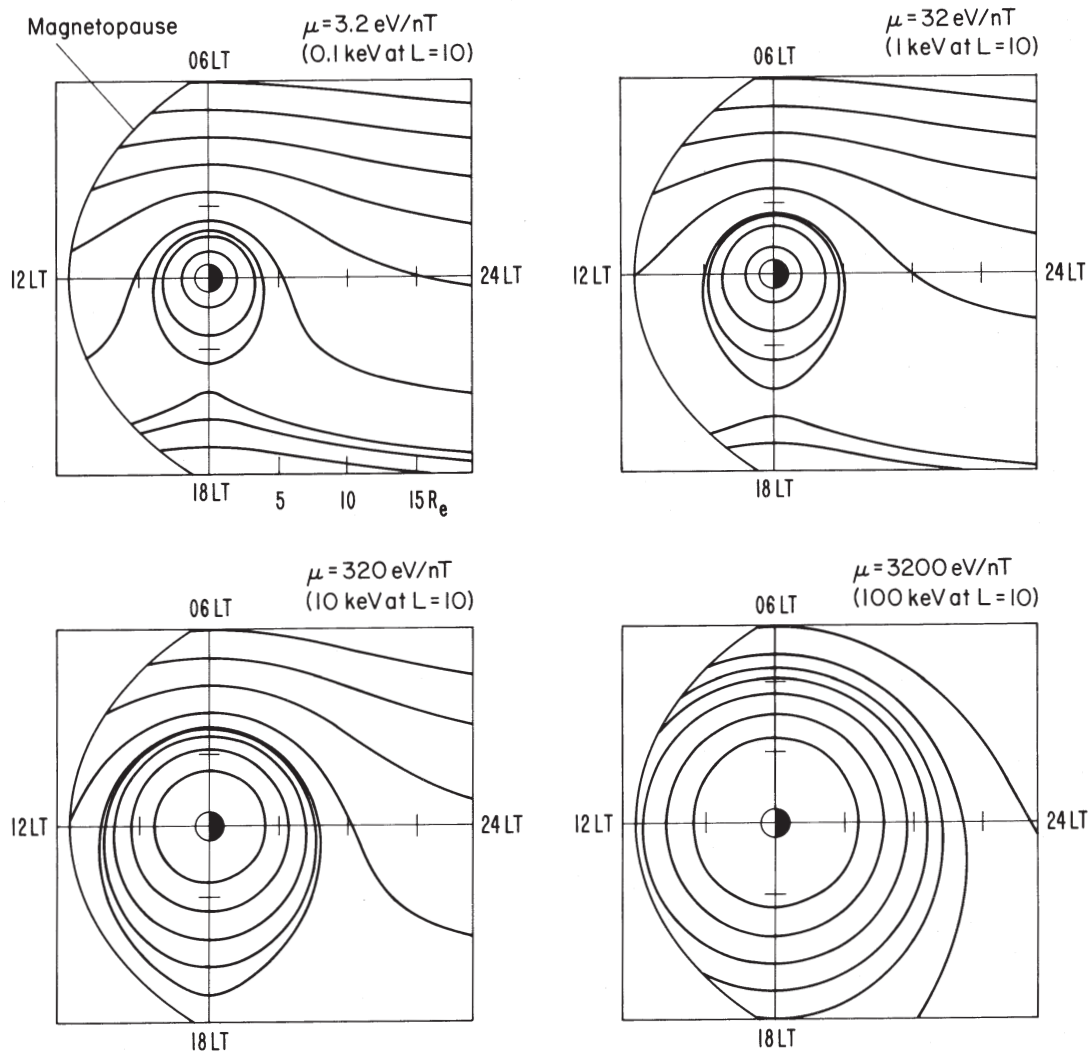
HYDRA's energy range and the range of magnetic field strengths encountered during an orbit allow for an almost complete coverage for a range of μ from 0.05 to 50.0 $\frac{\text{eV}}{\text{nT}}$.



Close to the Earth, high μ values are not measured, while further out low μ values are not measured.



D. Electron Drift Trajectories



from Lyons and Williams,
Quantitative Aspects of Magnetospheric Physics, 1984.



E. The (U,B.K) Theory

- Introduced by Whipple, *JGR*, 83, 4318–4326, 1978, also Sheldon, e.g. *GRL*, 20, 767–770, 1993.

- Total Energy: $W_{\text{tot}} = qU + \mu B_m$,

$$\Rightarrow \frac{\partial U}{\partial B_m} = -\frac{\mu}{q}. \quad (\text{straight lines !})$$

- Shielded cross-tail + corotation electric field: $U = -\frac{a}{r} - br^\gamma \sin(\phi)$,
Dipole magnetic field: $B = \frac{B_0}{r^3}$ (equatorial plane).

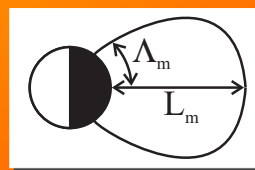
- Gussenhoven et al. (DMSP), *JGR*, 88, 5692–5708, 1983:

① Gussenhoven $\Rightarrow \Lambda_m(\text{Kp})$,

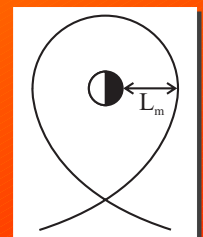
② Dipole $\Rightarrow L_m(\Lambda_m)$,

③ Electric Potential $\Rightarrow E_c(L_m)$.

① + ② + ③ $\Rightarrow E_c(\text{Kp})$



③



- Maynard and Chen (OGO 3+5), *JGR*, 80, 1009–1013, 1975:
 $E_c = 0.045 / (1 - 0.159 \text{ Kp} + 0.0093 \text{ Kp}^2)^3$ for $\gamma = 2$.



F. Description of plots

We performed field-line tracing for all points of the POLAR orbit for the period covered, to find the “equatorial” crossing point of that field line using the T87 magnetic field model with the correct Kp for each time.

“Equatorial” here means the GSM $z=0$ plane on the dayside, while on the nightside we found the points where the dot product between a vector from the center of the earth to the point on the field line and the magnetic field direction is zero. This effectively takes into account hinging in the tail region.

Particles were binned in μ and equatorial GSM x and y coordinates, for the following ranges of Kp:

0 to 0+

1- to 1+

2- to 2+

3- to 3+

4- to 4+

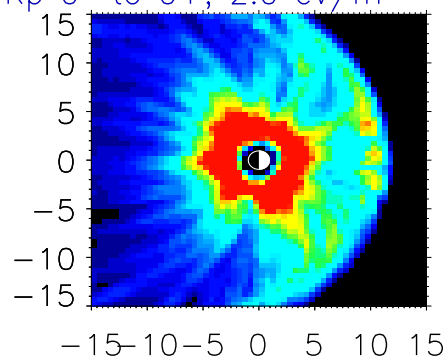
5- to 5+

6- to 9

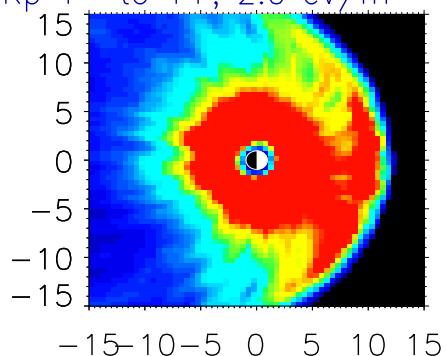
F1. HYDRA results Data Coverage



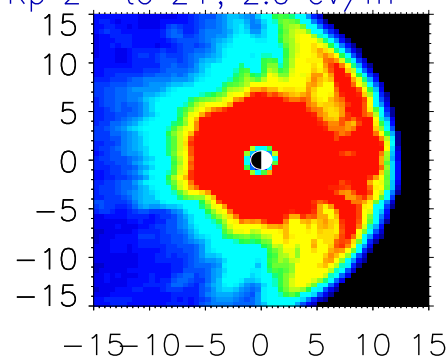
HYDRA i_all_1111
Kp 0- to 0+, 2.0 eV/nT



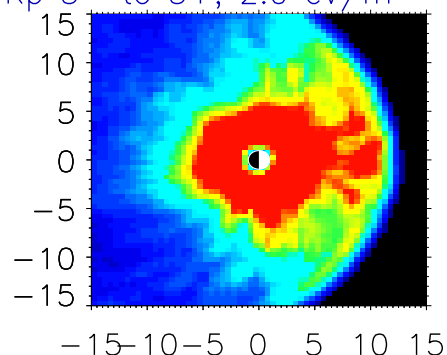
HYDRA i_all_1111
Kp 1- to 1+, 2.0 eV/nT



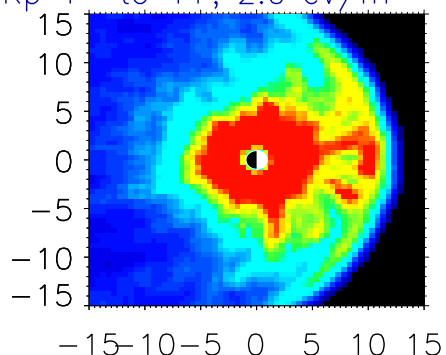
HYDRA i_all_1111
Kp 2- to 2+, 2.0 eV/nT



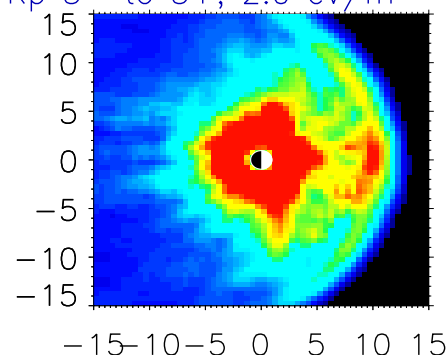
HYDRA i_all_1111
Kp 3- to 3+, 2.0 eV/nT



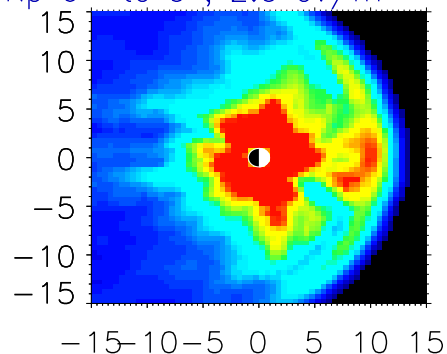
HYDRA i_all_1111
Kp 4- to 4+, 2.0 eV/nT



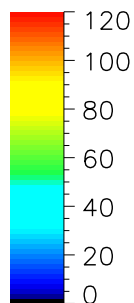
HYDRA i_all_1111
Kp 5- to 5+, 2.0 eV/nT



HYDRA i_all_1111
Kp 6- to 9, 2.0 eV/nT



samples

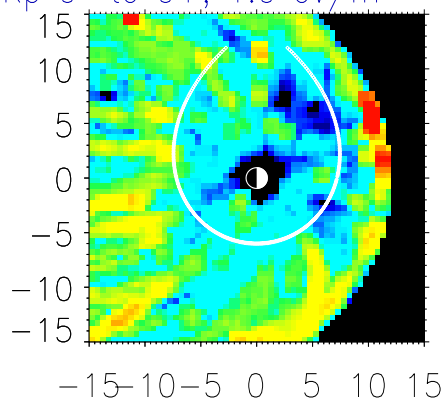


F2. HYDRA results

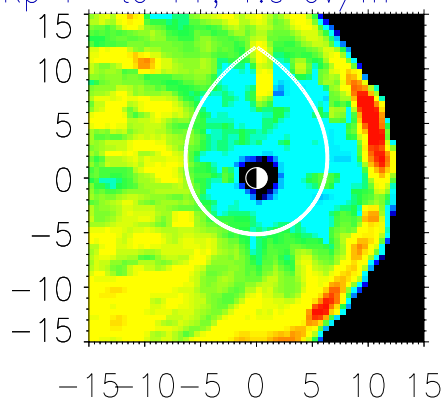
Electrons, $\mu = 1$ eV/nT



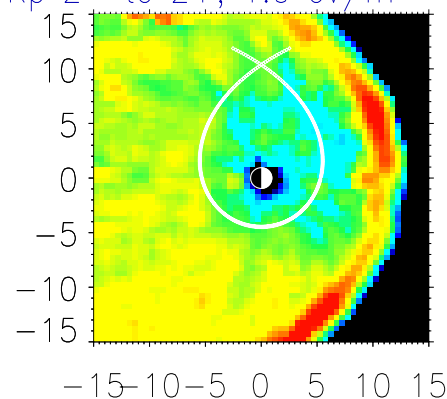
HYDRA e_all_1111
Kp 0- to 0+, 1.0 eV/nT



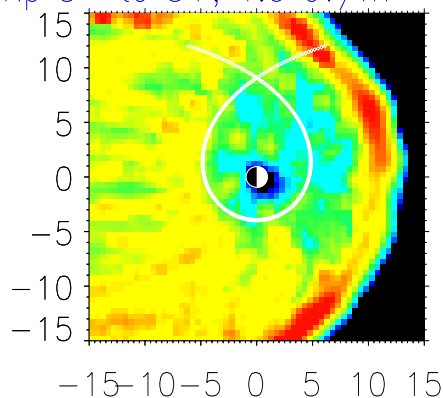
HYDRA e_all_1111
Kp 1- to 1+, 1.0 eV/nT



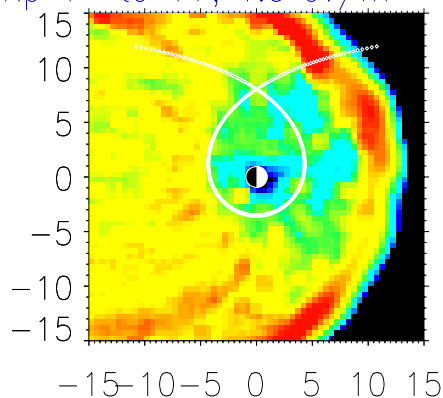
HYDRA e_all_1111
Kp 2- to 2+, 1.0 eV/nT



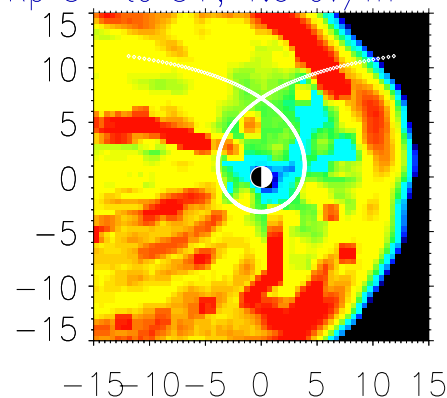
HYDRA e_all_1111
Kp 3- to 3+, 1.0 eV/nT



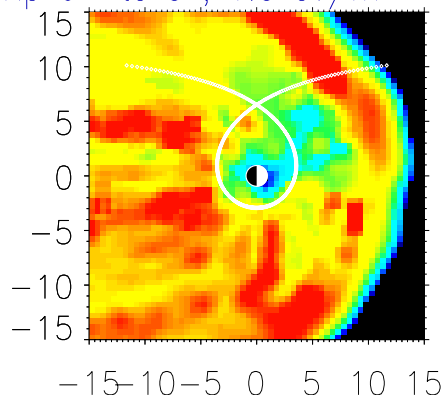
HYDRA e_all_1111
Kp 4- to 4+, 1.0 eV/nT



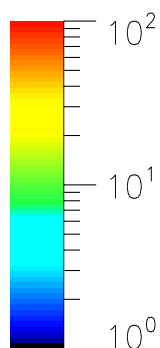
HYDRA e_all_1111
Kp 5- to 5+, 1.0 eV/nT



HYDRA e_all_1111
Kp 6- to 9, 1.0 eV/nT



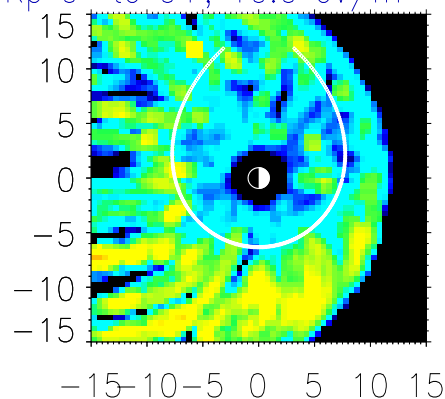
flux



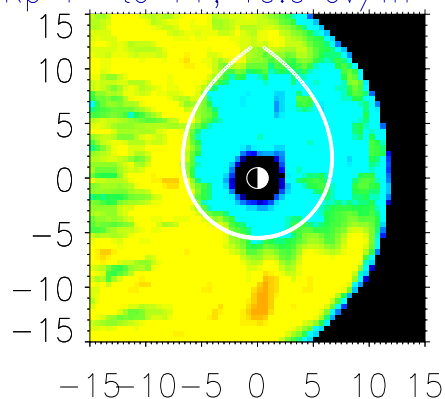
F3. HYDRA results Electrons, $\mu = 10$



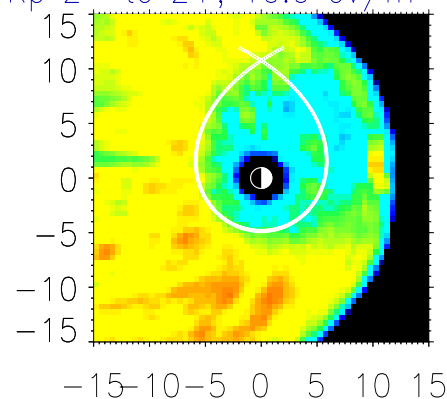
HYDRA e_all_1111
Kp 0- to 0+, 10.0 eV/nT



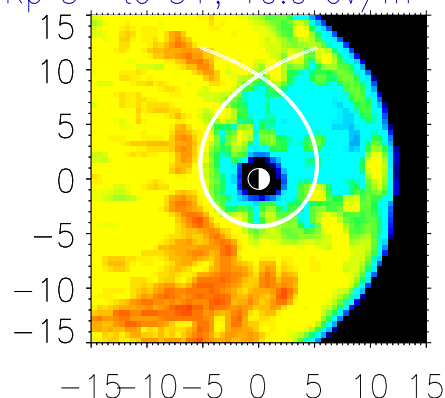
HYDRA e_all_1111
Kp 1- to 1+, 10.0 eV/nT



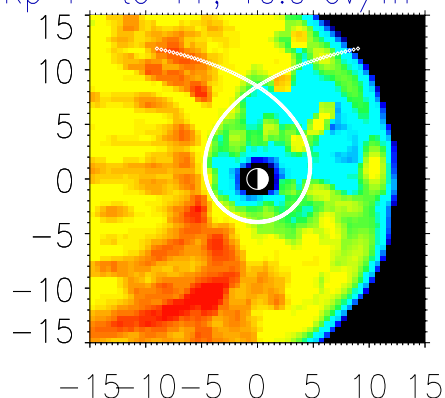
HYDRA e_all_1111
Kp 2- to 2+, 10.0 eV/nT



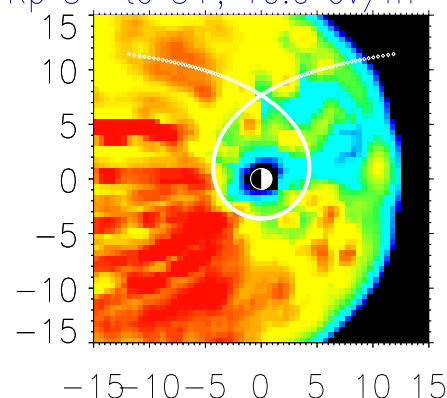
HYDRA e_all_1111
Kp 3- to 3+, 10.0 eV/nT



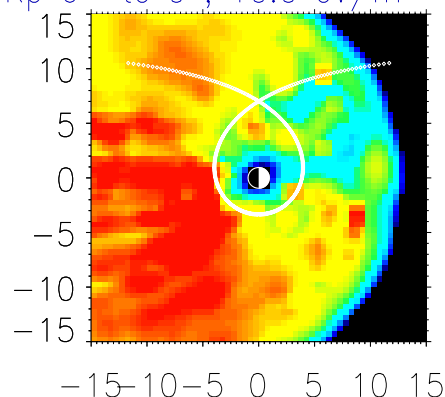
HYDRA e_all_1111
Kp 4- to 4+, 10.0 eV/nT



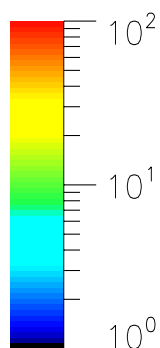
HYDRA e_all_1111
Kp 5- to 5+, 10.0 eV/nT



HYDRA e_all_1111
Kp 6- to 9, 10.0 eV/nT



flux

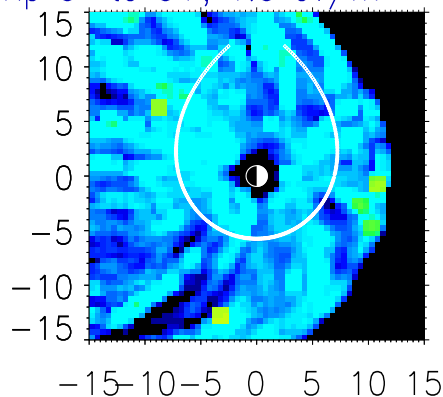


F4. HYDRA results

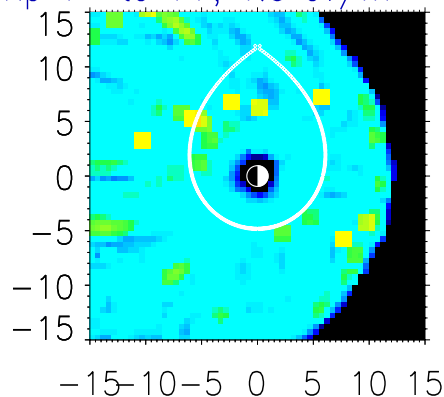
Ions, $\mu = 1$ eV/nT



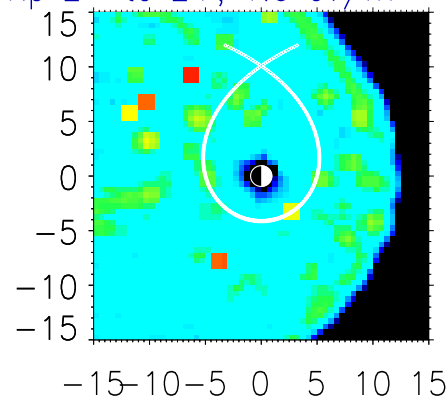
HYDRA i_all_1111
Kp 0- to 0+, 1.0 eV/nT



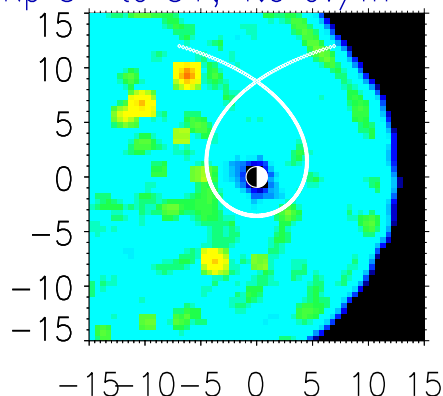
HYDRA i_all_1111
Kp 1- to 1+, 1.0 eV/nT



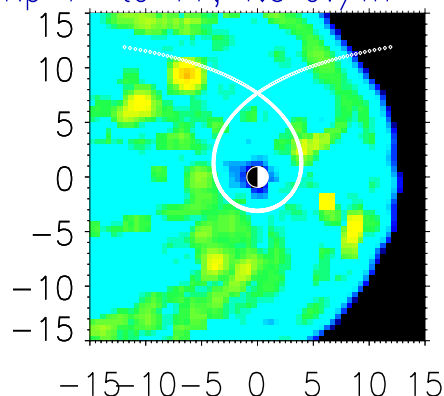
HYDRA i_all_1111
Kp 2- to 2+, 1.0 eV/nT



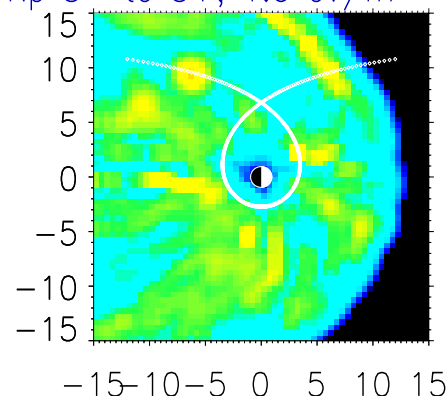
HYDRA i_all_1111
Kp 3- to 3+, 1.0 eV/nT



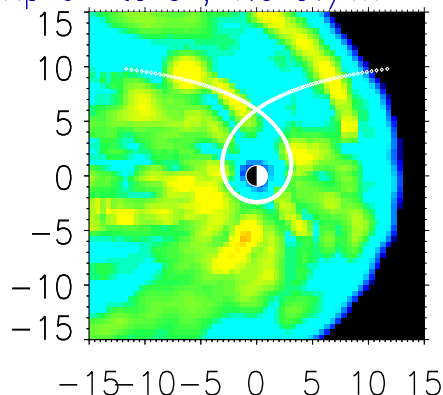
HYDRA i_all_1111
Kp 4- to 4+, 1.0 eV/nT



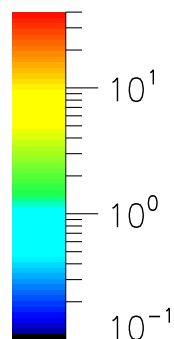
HYDRA i_all_1111
Kp 5- to 5+, 1.0 eV/nT



HYDRA i_all_1111
Kp 6- to 9, 1.0 eV/nT



flux

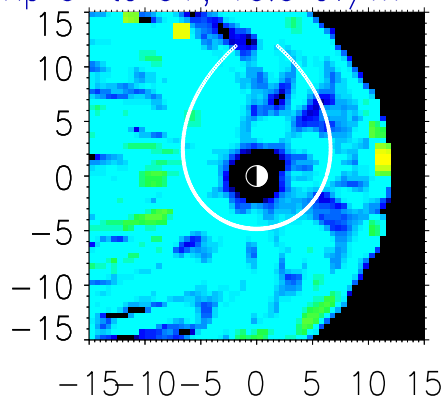


F5. HYDRA results

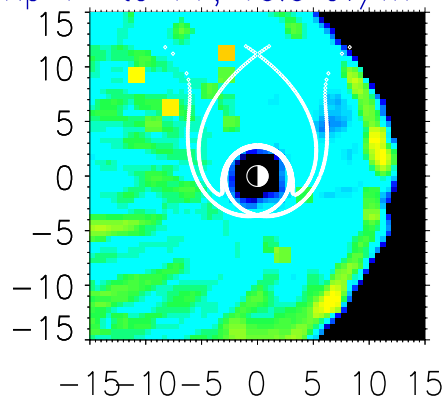
Ions, $\mu = 10$



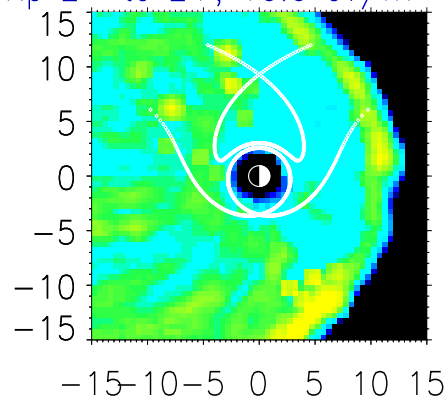
HYDRA i_all_1111
Kp 0- to 0+, 10.0 eV/nT



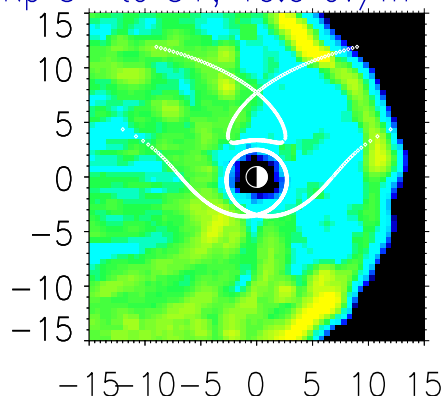
HYDRA i_all_1111
Kp 1- to 1+, 10.0 eV/nT



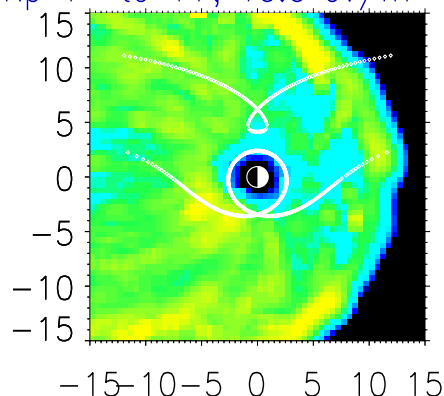
HYDRA i_all_1111
Kp 2- to 2+, 10.0 eV/nT



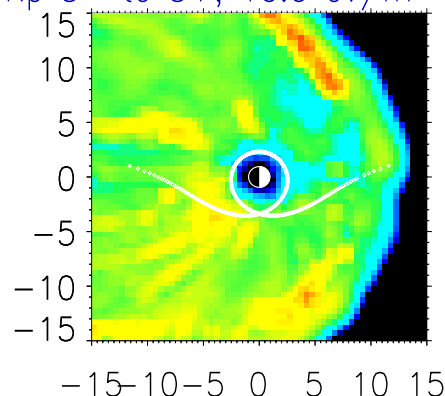
HYDRA i_all_1111
Kp 3- to 3+, 10.0 eV/nT



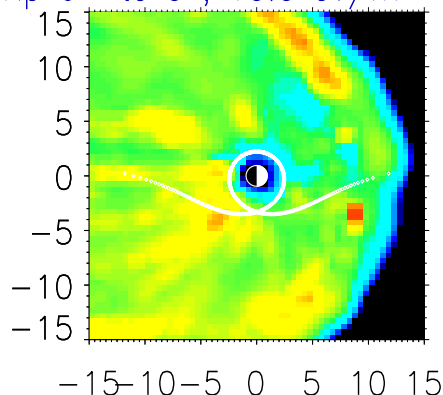
HYDRA i_all_1111
Kp 4- to 4+, 10.0 eV/nT



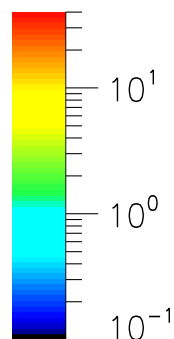
HYDRA i_all_1111
Kp 5- to 5+, 10.0 eV/nT



HYDRA i_all_1111
Kp 6- to 9, 10.0 eV/nT



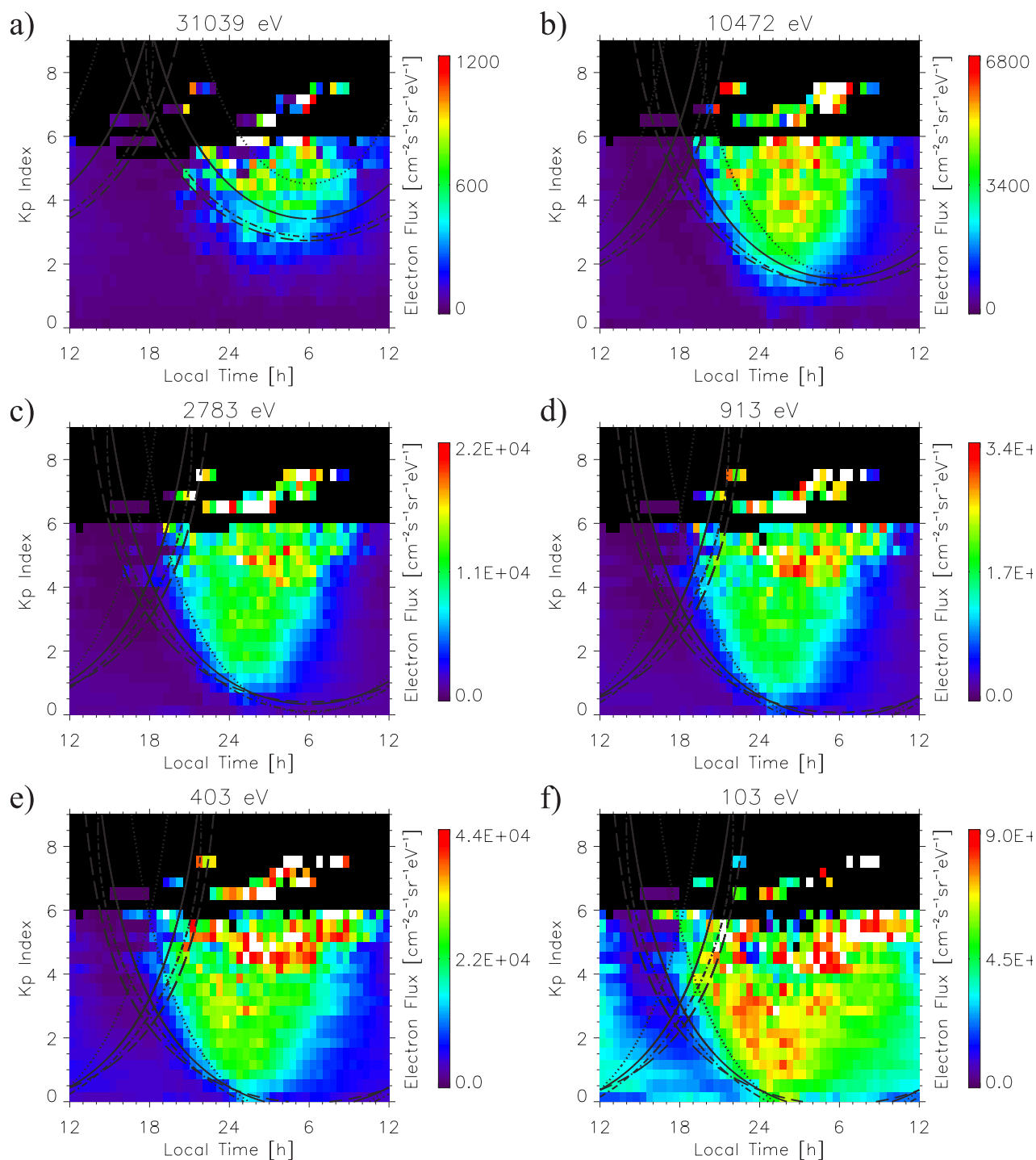
flux



F6. Geosynchronous comparison Geo MPA Electrons 1996

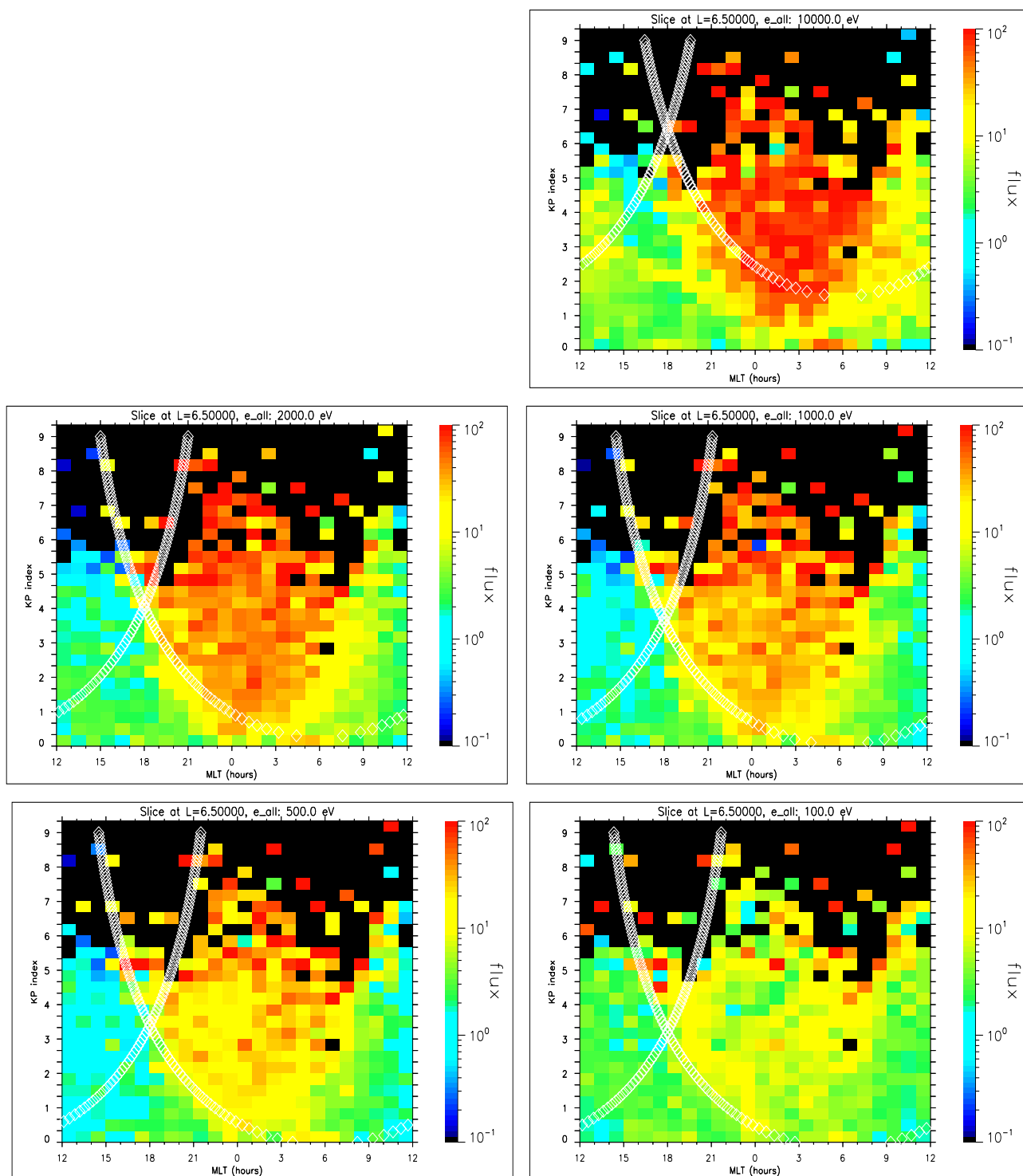


GEOSYNCHRONOUS ELECTRON FLUX 1996



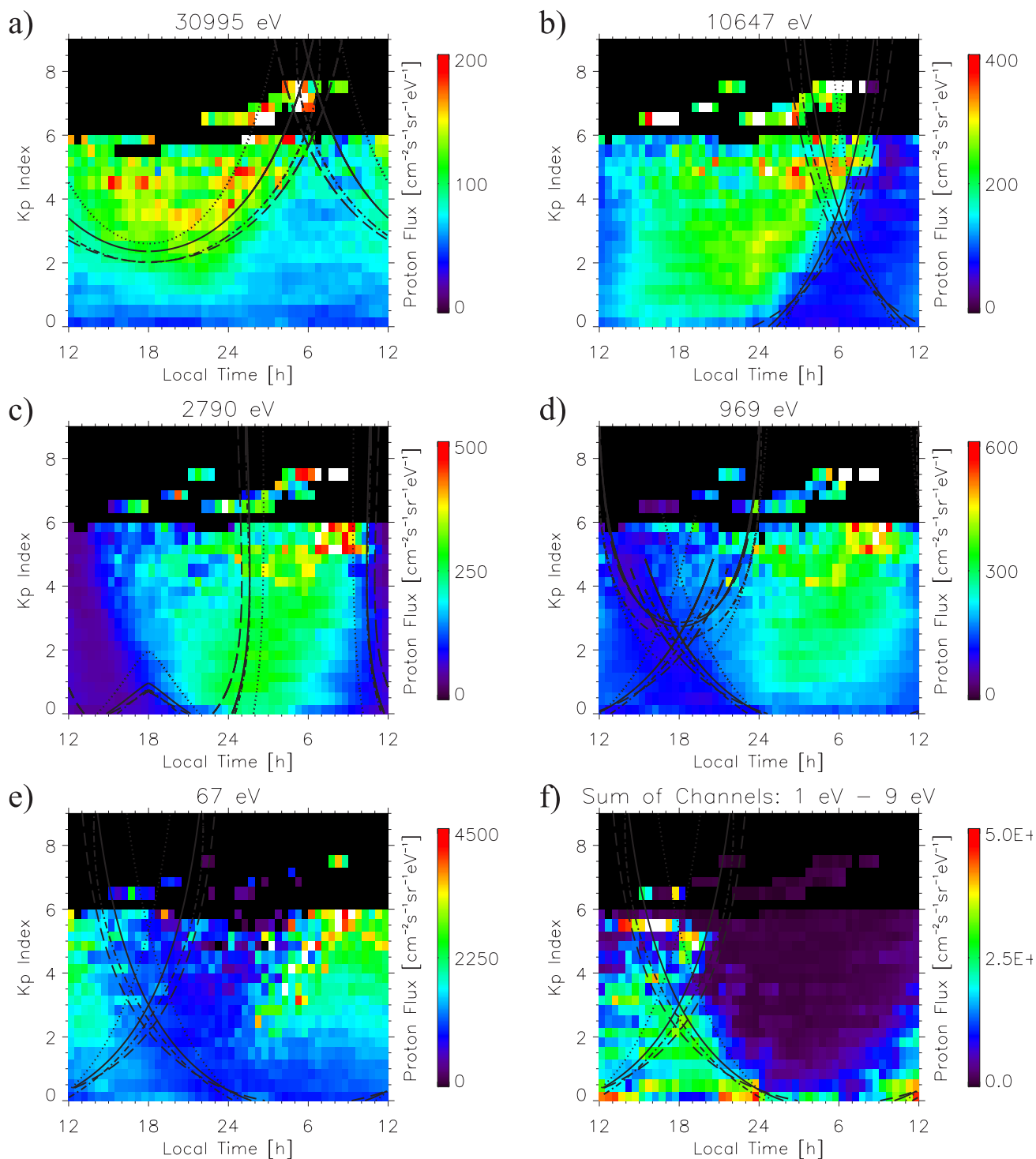
This work has been published by *Korth et al.* [1999]

F7. Geosynchronous comparison POLAR HYDRA Electrons



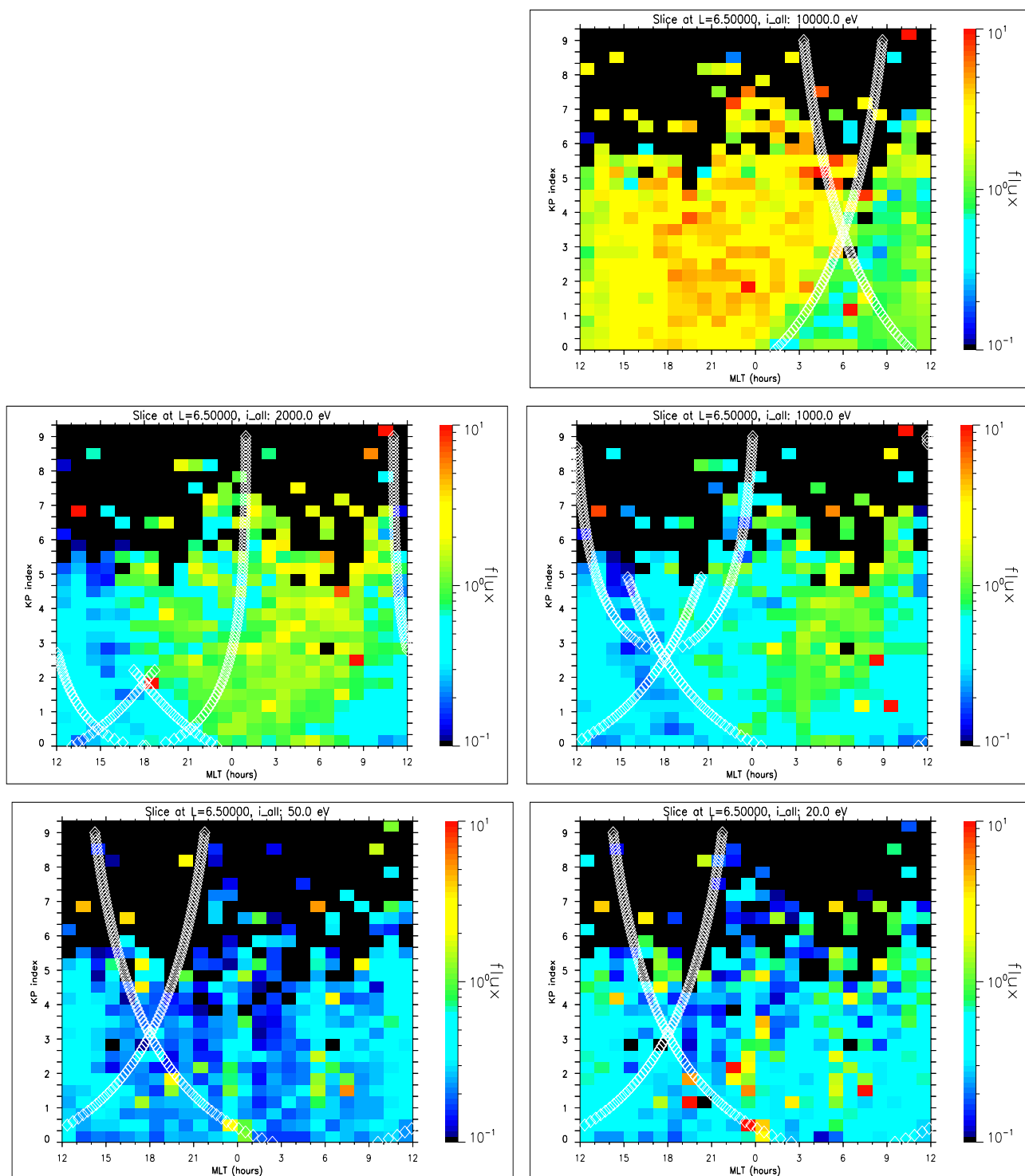
Energy channels are close to those for the MPA plots.

F8. Geosynchronous comparison Geo MPA Protons 1996



This work has been published by *Korth et al.* [1999]

F9. Geosynchronous comparison POLAR Hydra Protons



Energy channels are close to those for the MPA plots.



I1. Summary - Electrons

- POLAR can now provide global coverage of plasma sheet particles in the inner magnetosphere below $15 R_e$
- Electrons are very well organized by simple theoretical Alfvén boundaries.
- Lower μ electrons can penetrate deeper into the magnetosphere
- All μ show increasing losses as they drift towards the dayside. The longer electrons drift, the more they can be lost by wave-particle interaction. At higher Kp particles can drift around the dayside further.
- Kp dependence of Alfvén boundaries agrees very well with data. Electrons access is therefore primarily controlled by large-scale dawn-dusk electric fields, which show a simple dependence on Kp.
- Geosynchronous “slice” from HYDRA shows excellent agreement with previous study using LANL geosynchronous data only, but with increased noise due to the smaller database.



I2. Summary - Ions

- Ion data in General does not organize as well as the electron data.
- Ion drift orbits are more complex since co-rotation and dawn-dusk drift effects are opposite.
- Low energy particles have similar Alfvén boundaries like electrons, but do not organize along this boundary - there seems to be fairly uniform access everywhere. Possible ionospheric source or some other form of mixing? Only at high Kp fresh plasma from the plasmasheet organizes along the Alfvén boundary.
- Higher energy ions show a transition with KP from having Alfvén boundaries being asymmetric at dawn to being asymmetric at dusk. Again ions tend to be better organized by the Alfvén boundary for higher Kp.
- Geosynchronous “slice” from HYDRA shows excellent agreement with previous study using LANL geosynchronous data only, but with increased noise due to the smaller database.

J. References



Korth, H., M. F. Thomsen, J. E. Borovsky, and D. J. McComas, Plasma sheet access to geosynchronous orbit, *J. Geophys. Res.*, *104*, 25,047–25,061, 1999.

Scudder, J., et al., Hydra - a 3-dimensional electron and ion hot plasma instrument for the POLAR spacecraft of the GGS mission, *Space Sci. Rev.*, *71*, 459–495, 1995.